

A new prediction model of battery and wind-solar output in hybrid power system

Farzaneh Mirzapour¹ · Mostafa Lakzaei² · Gohar Varamini³ · Milad Teimourian^{4,5} · Noradin Ghadimi⁶

Received: 31 December 2016 / Accepted: 15 October 2017
© Springer-Verlag GmbH Germany 2017

Abstract In this paper short term power forecast of wind and solar power is proposed to evaluate the available output power of each production component. In this model, lead acid batteries used in proposed hybrid power system based on wind-solar power system. So, before the predicting of power output, a simple mathematical approach to simulate the lead–acid battery behaviors in stand-alone hybrid wind-solar power generation systems will be introduced. Then, the proposed forecast problem will be evaluated which is taken as constraint status through state of charge (SOC) of the batteries. The proposed forecast model includes a feature selection filter and hybrid forecast engine based on neural network (NN) and an intelligent evolutionary algorithm. This method not only could maintain the SOC of batteries in suitable range, but also could decrease the on-or-off switching number of wind turbines and PV modules. Effectiveness of the proposed method has been applied over real world

engineering data. Obtained numerical analysis, demonstrate the validity of proposed method.

Keywords Forecast engine · Lead acid battery · State of charge · Feature Selection

1 Introduction

By increasing the green energy installed capacity, the wind/solar power output prediction error precision provides serious challenge for researchers to the stable operation, dispatching as well as the safety and the quality insurance over power systems (Manla et al. 2010). On the other hand, to decrease such adverse effects on the power grid, wind-solar hybrid power generation system composed with storage batteries which have been used widely in several countries. It is clear that, once the battery's storage have been improved, the quality of output power can improved well.

Also, beside of the mentioned problems, the prediction of battery's behavior is an important problem in hybrid power systems based on solar-wind and battery (Loia et al. 2017; Abedinia and Ghadimi 2013; Meissner and Richter 2005; Akbary et al. 2017). Although the batteries have been used widely in power systems, their electrochemical reactions hides an unexpected complexity.

Recently, different methods have been introduced for simulation of battery behavior, which includes various degrees of complexity and simulation quality. Moreover, different battery behavior prediction models have been carried out. Where, the lead–acid batteries used in the hybrid solar–wind power generation systems are proposed to penalizing operating situation (Manla et al. 2010; Karden et al. 2007; Eskandari Nasab et al. 2014; Ghadimi and Firouz 2015). In Valenciaga and Puleston (2005), comprehensive

✉ Noradin Ghadimi
n.ghadimi@iauardabil.ac.ir

¹ Department of Computer Science, Faculty of Mathematics and Computer, Shahid Bahonar University of Kerman, Kerman, Iran

² Department of Electrical Engineering, Chabahar Maritime University (CMU), Chabahar, Iran

³ Department of Electrical Engineering, Beyza Branch, Islamic Azad University, Beyza, Iran

⁴ Sama Technical and Vocation Training College, Parsabad Moghan Branch, Islamic Azad University, Parsabad Moghan, Iran

⁵ Young Research and Elite Club, Germe Branch, Islamic Azad University, Ardabil, Iran

⁶ Young Researchers and Elite club, Ardabil Branch, Islamic Azad University, Ardabil, Iran

supervisor control model is proposed to regulate the output power wind-solar-batteries system to follow different load demand as well as maintain state of charge in batteries. In Datta et al. (2011), to improve the life time of batteries and the maintenance cost, an algorithm is proposed for a PV–diesel hybrid system to choose the optimal battery capacity. In Noruzi et al. (2015), fuzzy multi-objective optimization problems have been proposed by authors to decrease the cost of production and pollution in a wind-solar hybrid power system through reliability and environmental benefit. Combination of heat and power systems with storage battery system is presented in Milo et al. (2009) for hybrid-power micro-grid system to improve the reliability in stand-alone mode and economic exploitation in grid-connected mode. In Zou et al. (2014), the short-term power prediction of wind and solar power is utilized to quantify the available output power of each generation component, which is taken as constraint conditions of optimization problem with state of charge (SOC) of the batteries.

1.1 Contribution of paper

In this paper, we proposed a new hybrid forecast method for battery's behavior as well as the wind and solar power output. Currently, different prediction models have been presented to increase the wind power prediction accuracy, however because of limitation of the forecast technology and the characteristics of the wind volatility and complicated behavior of solar energy, an accurate prediction model is still demanded.

This article, proposed a hybrid power system based on wind-solar and battery. At first the proposed hybrid system is introduced and then, a new stochastic search algorithm is presented for minimizing the number of on/off-off/on switching of wind turbines and PV modules and maximize the utilization of the regulation capability of wind turbines, particularly, the predicted power of wind and solar is taken as generation ability of wind turbine and PV module. The prediction model is based on a feature selection which deals with mutual information (MI) and interaction gain (IG) of features, neural network (NN) based feature selection and a new stochastic search algorithm which optimized the NN based forecast engine. Beside of this presentation, a model of battery is presented. Obtained results proof that the use of the proposed method cause a significant improvements in tracking the actual desired demand, and a bulk decrease of on/off-or-off/on switching number of wind turbines.

So, the contribution of this paper can be summarized as:

1. A prediction model of battery behavior is presented based in stand-alone hybrid wind-solar power generation systems

2. A new enhanced stochastic search algorithm has been proposed which is based on shark smell optimization (ESSO) algorithm.
3. An accurate forecast engine is presented based on NN and ESSO.

1.2 Organization

The remaining parts of paper can be presented as follows. Sect. 2, presents the proposed hybrid power system based on wind-solar and battery. The proposed prediction method is presented in Sect. 3. Section 4, introduces the new stochastic search algorithm. Numerical analysis are presented in Sect. 5. Section 6 concludes the paper.

2 Hybrid wind–solar battery power system

The proposed hybrid power system includes three main simulation of wind-solar and battery. In this section we introduce each simulation. And at the end the structure of battery behavior is presented (Manla et al. 2010). For some system data, we used from other papers such as Manla et al. (2010). The modeling of proposed system is given as:

2.1 Wind power system model

In wind power system the blade tip speed ratio as well as blade pitch angle, are important sections which can be formulated as:

$$P_{wt} = \frac{1}{2} C_p(\lambda, \beta) A \rho v^3 \quad (1)$$

where P_{wt} is the mechanical power extracted which is related to the wind turbine rotor, ρ the air density, A presents the swept area of the rotor and finally, C_p introduces the power coefficient which defines the rotor aerodynamics as a function of both tip speed ratio. In this equation, λ , is the pitch angle of the rotor blades, β . Where, the tip speed ratio can be presented as the ratio among the blade tip speed and the wind speed as follow:

$$\lambda = \frac{\omega_r R}{v} \quad (2)$$

where ω_r is rotor speed and R is radius of the wind turbine rotor.

The power extracted from the wind is maximized when the rotor speed is such that C_p in Eq. (1) is maximized, which occurs for a determined tip speed ratio. Therefore, the control system of wind turbine is able to assure that maximizes the output power for a wide range of wind speeds, according to the optimum power extraction curve (Loia et al. 2017).

2.2 Photovoltaic model

The PV module is an important factor in solar power generation where its mathematical modeling is presented in the following where, in this system, the output terminals of the circuit are connected to the load where its voltage current equation of the PV module as:

$$I_{pv} = I_{ph} - I_0 \left[\exp \left(\frac{V_{PV} + I_{PV}R_s}{n_s m V_t} \right) - 1 \right] - \frac{V_{PV} + I_{PV}R_s}{R_p} \tag{3}$$

And

$$V_t = \frac{kT_c}{q} \tag{4}$$

where, I_{pv} introduce the output current of PV module, I_{ph} introduce the photo current, I_0 is diode reverse saturation current, V_{pv} presents the output voltage of PV module, R_s presents the series resistance, n_s presents the number of cells in series, m defines the diode ideality factor, V_t defines the thermal voltage, R_p defines the shunt resistance, k defines the boltzmann constant, T_c is boltzmann constant and q is electron charge (Eskandari Nasab et al. 2014).

Moreover, the photo current I_{ph} is evaluated by the solar irradiance G_c , module temperature T_c , as well as temperature coefficient α comprehensively. Where we can write:

$$I_{ph} = \frac{G_c}{G_r} [I_{cc} + \alpha(T_c - T_r)] \tag{5}$$

where G_r defines the standard solar irradiance, T_r represents standard temperature, and I_{cc} introduce short circuit current to standard irradiance and temperature. And the diode reverse saturation current I_0 is determined by the diode ideality factor m , standard temperature T_r , standard temperature T_c , module temperature T_c , and thermal voltage V_t . Where:

$$I_0 = I_{0r} \left(\frac{T_c}{T_r} \right)^{3/m} \exp \left[\frac{V_g(T_c/T_r - 1)}{mV_t} \right] \tag{6}$$

I_{0r} presents the reverse saturated current for standard temperature and V_g defines the energy gap. The power output of a PV module could be presented as:

$$P_{PV} = V_{PV} I_{PV} \tag{7}$$

where I_{PV} is output current, V_{PV} is operating voltage of PV module, and P_{PV} is output power of PV module.

2.3 Prediction model of battery behavior

In this paper the lead-acid battery has been considered in hybrid power system. These kinds of batteries includes two characteristics as state-of-charge (SOC) and the floating charge voltage (or the terminal voltage). Where, the SOC model is improved according to the hour counting method to simulate the lead-acid battery SOC behaviors in this paper (Buller et al. 2003). However, because of some errors in this method measurement, the floating charge voltage model will be considered in this simulation.

2.3.1 Model of battery state-of-charge

The problem of battery SOC is an important key in all batteries applications but, an accurate model is needed to prevent some drawbacks such as; not fully charged, over-discharged, or overcharged, etc (Gollou and Ghadimi 2017). In this paper, the ampere hour counting method, is considered for the mentioned SOC calculation. In this model the charge or discharge time and the current value can be evaluated as:

$$SOC = SOC_0 + \int_{t_0}^t \left(\frac{I_{bat}}{C_{bat}} \right) d\tau \tag{8}$$

where SOC_0 presents the battery SOC of the starting point; t and t_0 are the time of interest and the time of the starting point, respectively, I_{bat} is the battery current, C_{bat} defines the battery capacity. Furthermore, by considering the losses occur during battery charging and discharging as well as during storing periods the SOC can be evaluated as:

$$SOC = SOC_0 \left[1 - \frac{\sigma}{24}(t - t_0) \right] + \int_{t_0}^t \left(\frac{I_{bat} \eta_{bat}}{C_{bat}} \right) d\tau \tag{9}$$

where σ is the self-discharge rate, η_{bat} presents the battery charging and discharging efficiency. According to all chemical procedures, the battery capacity C_{bat} is temperature dependent which can be evaluated as:

$$C_{bat} = C'_{bat} (1 + \delta_c(T_{bat} - 298.15)) \tag{10}$$

where C_{bat} is the available or practical capacity of the battery through the battery temperature of T_{bat} ; C'_{bat} defines the battery's nominal capacity (Usman Iftikhar et al. 2006). In the proposed hybrid power system, to cover the load demand three resource components are considered as PV module, wind turbine and battery. In this paper we neglect the cable losses, so, we can write the battery current I_{bat} as:

$$I_{bat} = \frac{P_{Solar} + P_{Wind} \eta_{rectifier} - P_{Load} / \eta_{inverter}}{V_{bat}} \tag{11}$$

where the power of the PV array, wind turbine, and load are presented by P_{Solar} , P_{Wind} , and P_{Load} , respectively. V_{bat} represents the battery voltage. In this study the rectifier is used to transform the AC power from the wind turbine to DC.

2.3.2 Model of battery floating charge voltage

In this paper, model of battery floating charge voltage simulated by the equation-fit method, which can be presented as:

$$V'_{bat} = a(SOC)^3 + b(SOC)^2 + c(SOC) + d \tag{12}$$

where V'_{bat} is the battery floating charge voltage which can be presented based on temperature effect on battery voltage predictions (dT):

$$V_{bat} = V'_{bat} + \delta_V(T_{bat} - 298.15) \tag{13}$$

where V_{bat} is the calibrated voltage of the battery based on temperature effects. Also, the δ_V temperature coefficient is considered as -4 . Also, the presented parameters in (12) can be calculated as:

$$\begin{pmatrix} a \\ b \\ c \\ d \end{pmatrix} = \begin{pmatrix} a_1 & a_2 & a_3 \\ b_1 & b_2 & b_3 \\ c_1 & c_2 & c_3 \\ d_1 & d_2 & d_3 \end{pmatrix} \begin{pmatrix} I_{bat}^2 \\ I_{bat} \\ I \end{pmatrix} \tag{14}$$

where the $a_1, \dots, a_3, \dots, d_1, \dots, d_3$ are to be determined based on Least Squares Fitting method. In the following the battery charging test results in different currents is presented in Fig. 1. Also, the same figure is presented for discharging process as shown in Fig. 2.

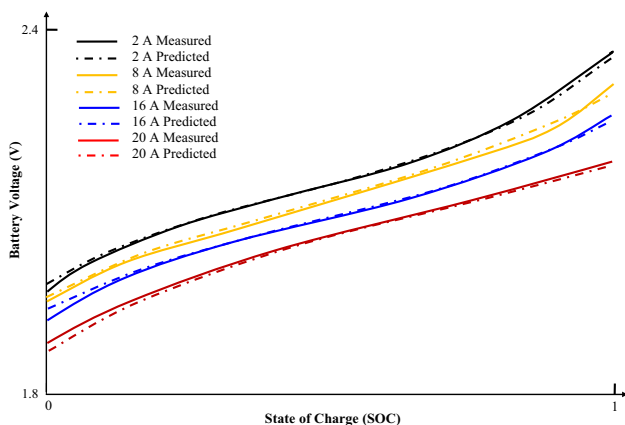


Fig. 1 Battery charging validation of the floating charge voltage model

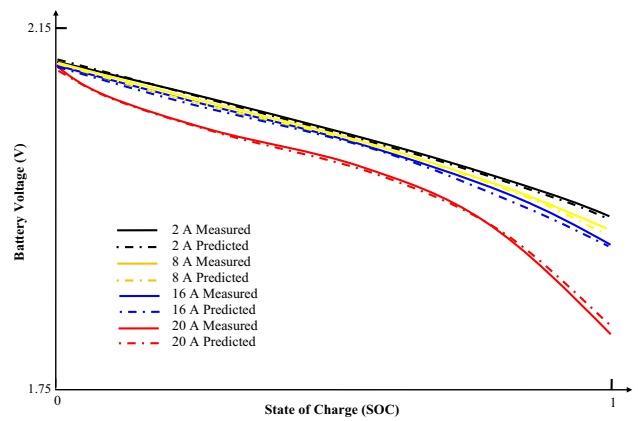


Fig. 2 Battery discharging process at different currents

3 Short-term power prediction for wind and solar power

In the following the schematic of active power control is presented in Fig. 3, which is based on power output that defines the sum of wind, photovoltaic and battery power generations (Le Mehaute and Crepy 1983; Jalili and Ghadimi 2016; Fang et al. 2012). The mentioned sum of power output in power system is evaluated based on dispatching power, the desired output power frequency, as well as power ramp rate limit. After that, the referred power facility to every wind turbine, PV module as well as battery based on running condition and the available active power, which is the predicted power from the block of short-term power prediction. In the next section, proposed forecast engine will be introduced which highlighted in Fig. 3.

3.1 The forecast engine structure

In whole process of forecast first, the input signal should be filtered to provide a well signal for estimation model, hence, we used two stage feature selection based on the information theoretic criteria of mutual information (MI) and interaction gain (IG). This model includes two cascaded filters to sift the irrelevant and redundant candidate features, respectively. Only the relevant non-redundant applicant inputs, organizing a minimum subset of the most revealing features for predicting the output adjustable, are selected by the feature selection policy. As this feature selection technique is not the focus of this paper, it is not further conversed here. The concerned reader can refer to (Fang et al. 2012) for specifics of this method.

After feature selection, the forecast engine will receive the signal to predict. It is clear that mixture of dissimilar neural networks (NNs) can hypothetically rise their learning abilities in a complex technique (Fang et al. 2012; Ghadimi et al. 2016; Liu et al. 2017; Kumar Aggarwal

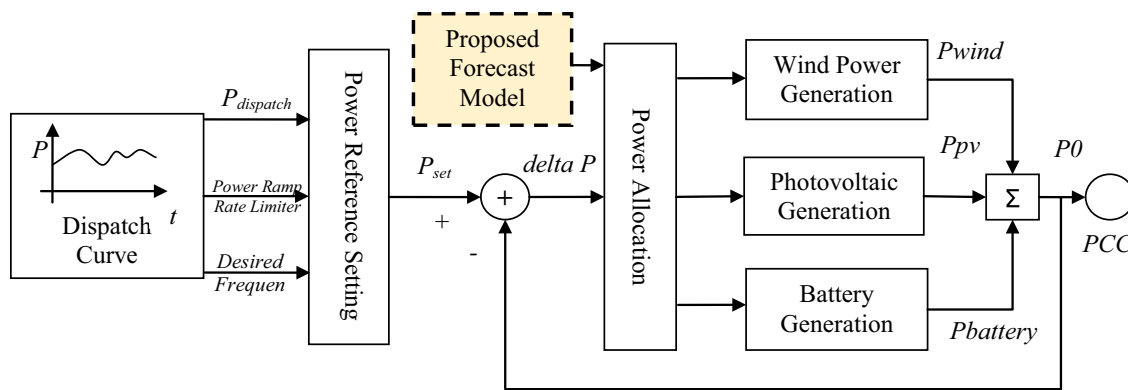


Fig. 3 Schematic of active power control

et al. 2009). But, in these methods the input data shared among their building blocks which means the mature sharing among the NN blocks. To attack the mentioned problem, a new method is introduced in this paper which includes three main stages. Before the forecast engine, a new section as preforecast will be presented which tracks a nonstationary signal with rapid variations. Where, if the multi-layer perceptron (MLP) has a preliminary prediction following tendency of the target signal, so the learning tendency of signal in forecast engine can be so easy. Additionally, to augment the accuracy of the proposed preforecast, we used the new stochastic search procedure to optimize its weights.

All the mentioned forecast engine blocks includes MLP forecasters. The three NNs have LM (Levenberg–Marquardt) learning algorithm. Further deliberations mitigating these choices can be found in Amjady and Hemmati (2009). The proposed model, is an accurate and strong forecast engine and delivers decent forecast consequences for proposed signal. Furthermore, to tackle of the overfitting or underfitting problems, a new stochastic algorithm will be applied in this paper to evaluate the NNs weights (Tsekouras et al. 2006; Lam et al. 2012). Therefore, the proposed version of shark smell optimization (SSO) is realized to recover the values of three block NNs. Grouping of this technique surge the learning abilities of proposed forecast engine in extracting the input/output mapping function of a complex signal. When one of the NNs of the proposed forecast engine is stuck in a local minimum through the training phase, neither that NN nor the next ones may be able to leakage from this trap.

It is clear that the NNs and the ISSO constituent have the same training examples and validation samples such that the weights can be moved among them. Consequently, the improved SSO tries to better minimize the validation error of NNs after its training algorithm is terminated.

4 Improved shark smell optimization

4.1 Shark smell optimization

This recently algorithm, has newly proposed by Abedinia et al. (2014). This algorithm is based on diverse shark smell abilities for localizing the answer of optimization problem (prey). In sharks’ drive, the concentration of the odor is an important factor to guide the shark to the prey. While, the shark moves in the manner based on higher odor concentration. This distinguishing is used in the proposed SSO algorithm to determine the solution of an optimization problem. More details of this algorithm has been presented in Abedinia et al. (2014). In the following the improvement of this algorithm will be presented.

4.2 Improved shark smell optimization

In the proposed method we improved the abilities of global and local search of algorithm. Accordingly, initial population is divided into two equal groups as the global and local groups. If one of the proposed groups finds a better answer in the mentioned procedures, better results will be replaced by previous one. This mechanism demonstrate the good relationship between two mentioned groups to improve the abilities of proposed method (Abedinia et al. 2014; Ghadimi et al. 2013; Ahmadian et al. 2014).

4.2.1 Global search group

As mentioned, the classic version of SSO works with position and velocity of shark based on odors concentration. Once, the shark reaches the best odor particle (best answer in global search), the velocity of sharks reaches to zero, accordingly, the shark will be stop the search procedure.

Where, the premature convergence can be happen in local optima point.

So, in global search procedure, we proposed the non-stop (NS) technique, for improving the search abilities. In this model, after evaluating the shark’s velocity, if its velocity is less than μ , and the odor is not the best, a random number (R) will be generated between $[-R, R]$ and will be added to that velocity. This work cause reactivates the shark, and makes it take part in the search process, again. In early, iteration of algorithm, the value of R will be large amount, and by improving the processes value goes to smaller. Where, this random generation distributed in the interval $[0, 1]$ and the model of linearly decreasing R is expressed as follows:

$$R = (r_{ini} - r_{end}) \frac{(T - t)}{T} + r_{end} \tag{15}$$

where r_{ini} and r_{end} are the initial and final values for R , respectively. Also, T represents the maximum number of iterations and t defines the current iteration. After implementation of the mentioned method, the position of shark will be updated. By the mentioned technique, the diversity and search exploration of proposed algorithm will be increased and prevent the mature convergence.

4.2.2 Local search group

Although the obtained point in premature global search is not the best one but we can use this point for improving the local search exploration. In other words, appropriate

solutions are more likely to be found in neighborhood area of the point in global search, hence, we improve the local search exploration around the mentioned point. Accordingly, the proposed algorithm will not trap in local minima and it can resume the search process around the best point to find the better solution. Consequently, we replace the obtained results for the best point by the following point:

$$X^{new} \in [X^L, X^H]$$

$$X^L = X_i^{k+1} - \frac{R(X_i^{k+1} - x_{min})}{(x_{max} - x_{min})}$$

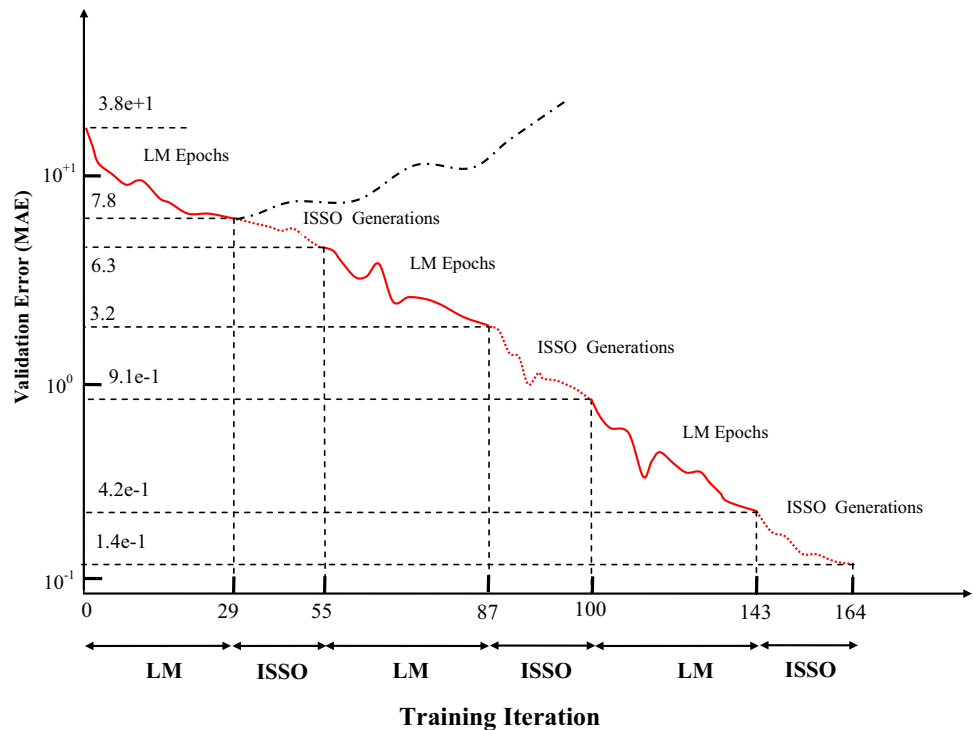
$$X^H = X_i^{k+1} + \frac{R(x_{max} - X_i^{k+1})}{(x_{max} - x_{min})} \tag{16}$$

Here, the X^{new} is chosen randomly between X^L and X^H . Also, x_{max} and x_{min} are the search space borders, and R is decreased linearly from 1 to 0 as:

$$R = \frac{T - t}{t} \tag{17}$$

By updating the velocity and location of shark, if the obtained point (optimization answer) is less than the global point, this point will be replaced with new point obtained and in the next iteration, the stochastic search will be done around the obtained new point, otherwise it will not change and the search process around this point will continue.

Fig. 4 Evaluated the training results (solid line) with proposed algorithm (dotted line) and a single LM learning algorithm (dashed-dotted line)



5 Numerical results

In this step the planned technique is applied over a real world engineering data. Earlier, presenting numerical results of this test case, an appropriate insight about the proposed forecast engine’s performance in the training phase, a typical curve based on its error and training is represented in Fig. 4. Where, mean absolute error (MAE) is considered as the error function.

Actually, to demonstrate the validity of proposed method on overfitting and untimely convergence problems this analysis is presented. By considering Fig. 4, it can be considered that, for each stage of proposed NN based forecast engine by increasing the error function the training process will stop by replacing the last parameters of weight (based on proposed optimization method). So, the LM half cycle of the first, second and third iterations has 29, 87 – 55 = 32 and 143 – 100 = 43 training epochs (pass through the entire training set), respectively, demonstrated by the early stopping model. Furthermore, proposed ISSO half cycle of the first, second and third iterations has 55 – 29 = 26, 100 – 87 = 13 and 164 – 143 = 21 generations, respectively, determined by the stopping criterions of the ISSO.

Additionally, to present a proper vision about the presentation of the proposed model of training mechanism, the first LM half cycle is continued after the early stopping point and represented by dashed-dotted line. Where we can claim the overfitting problem through this process. After trapping in a local minimum in this phase, the LM cannot escape from this point and this problem cause an overfitting. But, by proposed strategy, it is clear that this procedure is reduced monotonically in each presented stages based on combined model.

Also, in the following the proposed forecast strategy is applied over the historical data of wind speed and solar

irradiance gathered from Inner Mongolia which is used as real wind speed and solar irradiance during the simulation. The mentioned data has been presented in Fig. 5.

In this section the proposed ISSO implementation is considered in training mechanism. This algorithm is coupled with proposed forecast engine to avoid overfitting which is a serious problem in training process. By occurring the overfitting in training phase, obtained training error stays to reduction and it seems that the training process developments, while indeed the generalization proficiency of the forecast engine degrades and it fails its forecast skill for hidden forecast samples. But, as the prediction error is not accessible in the training stage, the error of validation sample is considered for its estimation. The obtained error from validation samples can be considered as prediction of forecast engine error for hidden prediction sample. This criteria is an appropriate metric tool for testing the forecast engine ability in overfitting problem. To improve the efficiency of validation error, its samples must be same as prediction samples where in this state the validation error can provide close estimate of the prediction error. In this paper, 50 days historical data for each forecast engine are divided in a training and validation subsets including the first 49 days (49 × 24 = 1176 h samples) for training and 1 day for validation samples are considered. By this model, the ISSO trained each forecast engine in proposed forecast engine structure. The proposed ISSO mechanism is considered as an optimization problem where the error of the constructed training samples or training error is considered as objective function. And the weights and neurons are considered as decision variables. First, the ISSO population is initialized randomly and the initial value for decision variables will be considered. In each iteration, the decision variables changes based on training error improvement. In final iteration, the evaluation process of validation error will done. Once, the validation error began to rise, the generality performance of forecast engine starts to reduce (the overfitting began to effect the training process) so, the training of forecast engine should be transferred to the matching iteration. Furthermore, the weights of forecast engine will be set based on decision variables due to the best individual of the optimization process of ISSO. So, the trained forecast engine can forecast the future values for the next horizon.

Also, for assessment the proposed technique accuracy diverse error criterions measured in this test case as; MAE, normalized mean absolute percentage error (NMAPE), root mean square error (RMSE). In the next, mathematical equation of these errors are presented:

$$NMAPE = \frac{100}{N} \sum_{i=1}^N \frac{|PV_i^f - PV_i^r|}{|PV_i^r|} \times 100\% \tag{18}$$

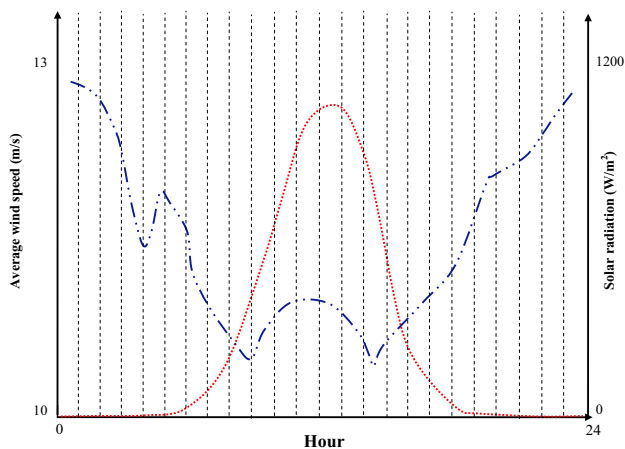


Fig. 5 Curve of wind speed and solar radiation; red dotted (PV), blue dashed-double dotted (wind)

where N is the total amount of data points; PV_i^f is the forecasted PV power data, PV_i^r is the real PV power data, and its average is presented by bar.

$$MAE = \frac{1}{N} \sum_{i=1}^N |PV_i^f - PV_i^r| \tag{19}$$

$$RMSE = \sqrt{\frac{1}{N} \sum_{i=1}^N (PV_i^f - PV_i^r)^2} \tag{20}$$

Also, for giving the fair comparison of proposed method with published works, all situations are considered in this paper same as (Ghadimi and Firouz 2015). Gained results for four seasons through the comparison with other techniques are presented in Table 1 through comparison of (Ghadimi and Firouz 2015). Also, this table has been presented as graphical analysis in Fig. 6. All of the presented results in this table are quoted directly from (Ghadimi and Firouz 2015). By considering to this table it can be considered that our proposed method could provide better results in all seasons for all error criterions.

As presented in Fig. 6, it can be considered that the proposed method provides minimum error in comparison with other well-known methods. In this figure, low space of

Table 1 Obtained results of proposed forecasting method through the comparison with other models

Methods	Error	Winter		Spring		Summer		Fall	
		23th Dec.	5th Dec.	12th May	27th Apr.	26th Jun.	27th Aug.	18th Oct.	28th Sep.
BPNN	NMAPE	29.65	35.47	18.55	23.45	21.05	18.67	15.17	32.74
	MAE	1.08	1.47	1.56	1.98	1.88	1.35	0.81	2.01
	RMSE	1.92	2.15	2.04	2.73	2.20	1.86	0.96	2.68
RBFNN	NMAPE	16.71	35.46	17.24	18.21	10.84	5.12	7.22	21.86
	MAE	0.61	1.47	1.45	1.54	0.94	0.37	0.38	1.34
	RMSE	0.74	1.72	1.94	2.20	1.43	0.45	0.49	1.80
WT + BPNN	NMAPE	11.94	30.26	16.99	17.95	17.62	5.98	13.07	22.44
	MAE	0.43	1.25	1.44	1.51	1.54	0.43	0.70	1.38
	RMSE	0.62	1.66	1.70	1.89	2.05	0.55	0.79	1.52
WT + RBFNN	NMAPE	8.16	13.81	8.91	13.14	8.54	4.25	4.32	12.17
	MAE	0.29	0.57	0.75	1.11	0.74	0.30	0.23	0.75
	RMSE	0.40	0.64	1.01	1.57	1.06	0.38	0.32	0.87
Proposed	NMAPE	6.77	10.20	6.52	10.21	5.94	3.10	3.03	9.47
	MAE	0.16	0.41	0.52	0.93	0.64	0.21	0.19	0.52
	RMSE	0.30	0.39	0.84	1.31	0.84	0.26	0.26	0.64

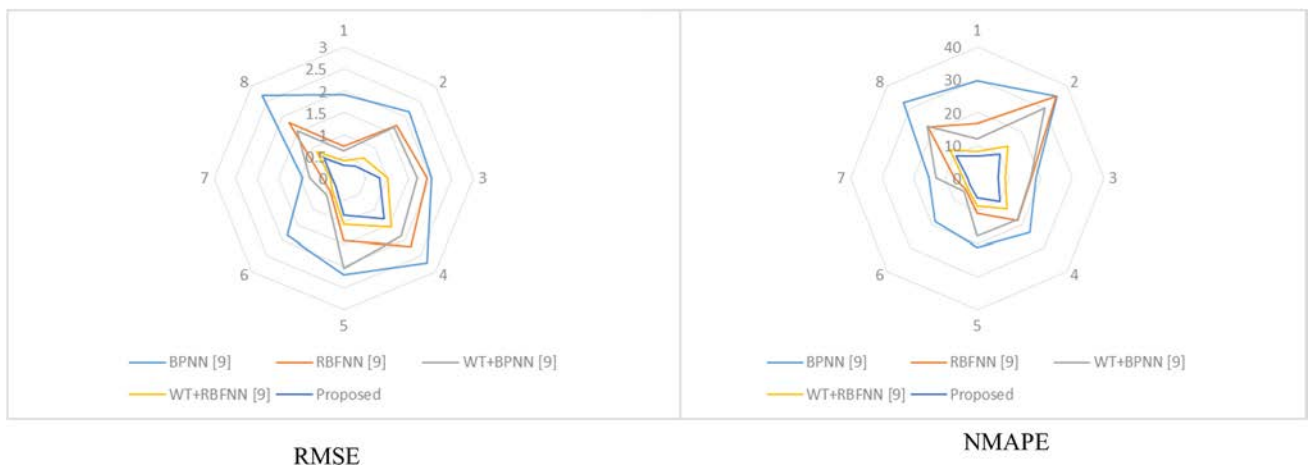


Fig. 6 Comparison of the proposed solar PV output forecast strategy with other methods

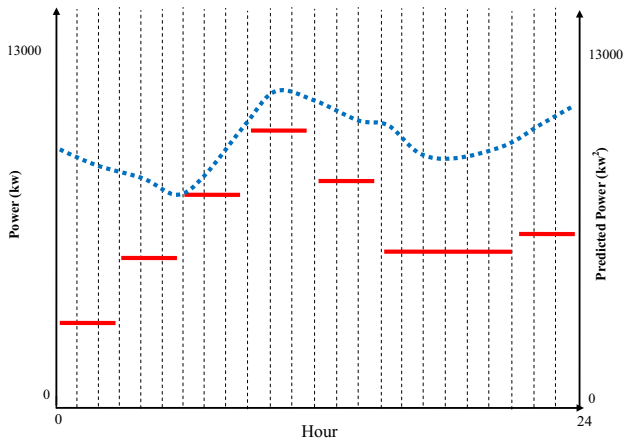


Fig. 7 Power control effects by the average method (red solid) power prediction (blue dotted)

curves means better accuracy and as presented in this figure the blue line space is the lowest space in comparison with other techniques.

To prove that the proposed active power allocation method outstripped the classical average technique, we assessed the efficacy of the proposed active power distribution for active power control to meet the power obligation of the power grid when the energy storing batteries were not complex in active power control (Case 1) or complicated in it (Case 2).

In first Case, the desired output for proposed composed strategy given by the upper power grid was a stair-wise signal as shown in Fig. 7, where the power levels were set at minimum in 2000 and maximum in 10,000 kW,

with transitions occurring at 3, 5, 10, 13, 15, and 20 h, respectively.

Furthermore, the proposed method of grid-connected constituent amount for wind turbines and PV modules has been other methods as presented in Fig. 8. Regarding to maximizing the operation of the directive ability of wind turbines, the PV modules did not control to start till the regulating ability of wind turbines was insufficient to satisfy the anticipated output power. So it seems that the grid-connected number of PV modules was non-zero where the grid-connected value of wind turbines was 8. As presented in this figure, on/off switching values of the proposed technique is less than that of the average model, clearly, in the whole sequence of simulation experimentation.

For the second case, the anticipated output for proposed complex model given by the upper power grid was a stair-wise signal as shown in Fig. 9, while the power levels were set at minimum 4000, and maximum 11,000, by transitions occurring at 3, 5, 11, 16, and 19 h, correspondingly. Such an output power request route was characteristic in daily operation of the complex model. The output of proposed complex

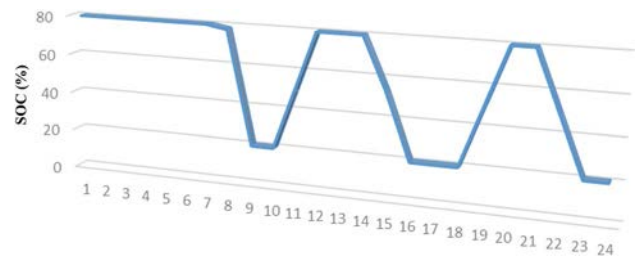


Fig. 9 SOC of the energy storage battery

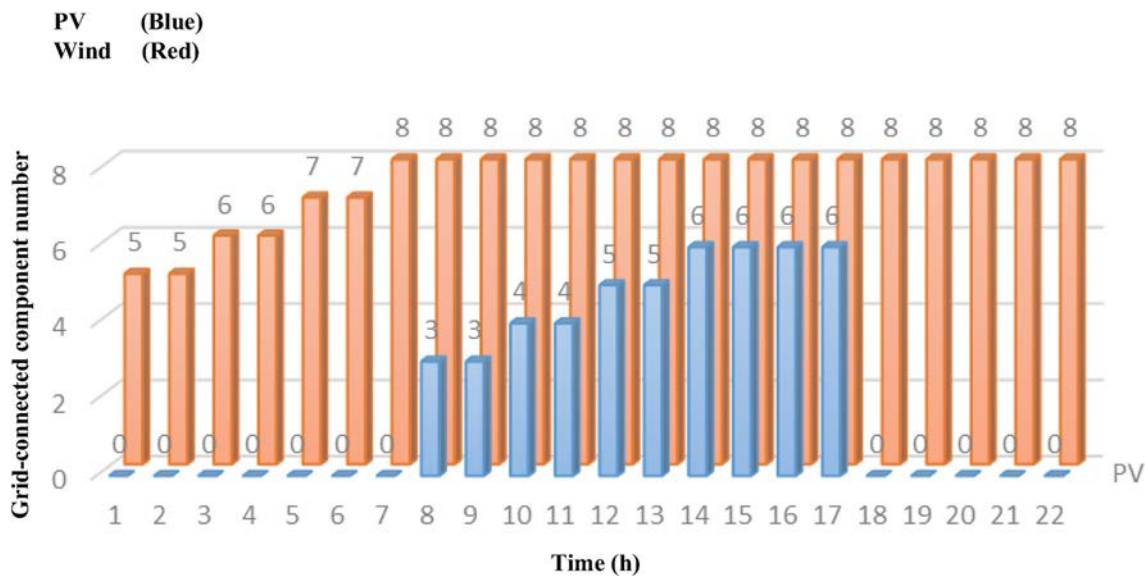


Fig. 8 Statistics of grid-connected component number by using the proposed method

model evaluated by using the power allocation method was associated with the anticipated output power in Fig. 9. As shown in this figure, once the sum of prediction power of the wind turbines and PV modules are more than the anticipated output power, the complex model output controlled by the proposed allocation technique could track the setting power, where the output power curve was without volatility and is smooth.

Formerly, once the total forecast power was under the anticipated output power, the energy storage batteries were controlled to discharge till the SOC of the energy storage batteries was equivalent to SOC_{min} , as presented in Fig. 9. So, output power of proposed complex model could track the setting power after discharging in the part where SOC was above SOC_{min} . Consequently, the wind power and PV modules were the maximum power output as the forecast power when SOC was under SOC_{min} to enhance the utilization rate of wind and solar energy resources for the machineries.

6 Conclusion

In this paper, an active power control strategy named complex control block has been presented through multi-objective algorithm. In this model, short-term wind and solar power have been forecasted through application of an intelligent method. In this model, feature selection, three stage forecast engine has been considered. Where, in this process all of the forecast engine stages have been optimized by SSO algorithm. Where, the weights of forecast engine optimized by this algorithm. Furthermore, the active power allocation has been considered as an optimization problem, and a decoration search algorithm has been considered to search the optimal explanation. Obtained results proof the validity of proposed method though improvement of active power output performance and decrease the fluctuation rate, and in a same time keep the maintain of SOC in batteries in an appropriate range. Furthermore, it could keep the maximization of utilization for regulation aptitude of wind turbines and decrease amount of on-or-off switching of wind turbines as well as PV modules.

References

- Abedinia O, Ghadimi N (2013) Modified harmony search algorithm based unit commitment with plug-in hybrid electric vehicles. *J Artif Intellect Eng* 2(6):49–62
- Abedinia O, Amjady N, Ghasemi A (2014) A new meta-heuristic algorithm based on shark smell optimization. *Complex J*. doi:10.1002/cplx.21634 2014.
- Ahmadian I, Abedinia O, Ghadimi N (2014) Fuzzy stochastic long-term model with consideration of uncertainties for deployment of distributed energy resources using interactive honey bee mating optimization. *Front Energy* 8(4):412
- Akbary P et al (2017) Extracting appropriate nodal marginal prices for all types of committed reserve. *Comput Econ* 1–26
- Amjady N, Hemmati M (2009) Day-ahead price forecasting of electricity markets by a hybrid intelligent system. *Eur Trans Electric Power* 19(1):89–102
- Buller S, Thele M, Karden E, De Doncker R (2003) Impedancebased non-linear dynamic battery modeling for automotive applications. *J Power Sources* 113(2):422–430
- Datta M, Senjyu T, Yona A et al (2011) Photovoltaic output power fluctuations smoothing by selecting optimal capacity of battery for a photovoltaic-diesel hybrid system. *Electric Power Components Syst* 39(7):621–644
- Eskandari Nasab M et al (2014) A new multiobjective allocator of capacitor banks and distributed generations using a new investigated differential evolution. *Complexity* 19(5):40–54
- Fang K, Mu D, Chen S, Wu B, Wu F (2012) A prediction model based on artificial neural network for surface temperature, simulation of nickel–metal hydride battery during charging. *J Power Sources* 208:378–382
- Ghadimi N, Firouz MH (2015) Short-term management of hydro-power systems based on uncertainty model in electricity markets. *J Power Technol* 95(4):265
- Ghadimi N, Afkousi-Paqaleh M, Nouri A (2013) PSO based fuzzy stochastic long-term model for deployment of distributed energy resources in distribution systems with several objectives. *IEEE Syst J* 7(4):786–796
- Ghadimi H, Akbarimajd A, Ghadimi N (2016) Optimal congestion management: strength Pareto gravitational search algorithm
- Gollou AR, Ghadimi N (2017) A new feature selection and hybrid forecast engine for day-ahead price forecasting of electricity markets. *J Intell Fuzzy Syst* 1–15 (Preprint)
- Jalili A, Ghadimi N (2016) Hybrid harmony search algorithm and fuzzy mechanism for solving congestion management problem in an electricity market. *Complexity* 21(S1):90–98
- Karden E, Ploumen S, Fricke B, Miller T, Snyder K (2007) Energy storage devices for future hybrid electric vehicles. *J Power Sources* 168(1):2–11
- Kumar Aggarwal S, Mohan Saini L, Kumar A (2009) Electricity price forecasting in deregulated markets: a review and evaluation. *Electr Power Energy Syst* 31(1):13–22
- Lam AYS, Li VOK, Yu JJQ (2012) Real-coded chemical reaction optimization. *IEEE Trans Evol Comput* 16(3):339–353
- Le Mehaute A, Crepy G (1983) Introduction to transfer and motion in fractal media: The geometry of kinetics. *Solid State Ion* 9/10:17–30
- Liu Y, Wang W, Ghadimi N (2017) electricity load forecasting by an improved forecast engine for building level consumers. *Energy*
- Loia V, Tomasiello S, Vaccaro A (2017) Joining fuzzy transform and local learning for wind power forecasting. In: Joint 17th World Congress of International Fuzzy Systems Association and 9th International Conference on Soft Computing and Intelligent Systems (IFSA-SCIS 2017), June 27–30, 2017, Otsu, Japan
- Manla E, Nasiri A, Rentel CH, Hughes M (2010) Modeling of zinc/bromide energy storage for vehicular applications. *IEEE Trans Ind Electron* 57:624–632
- Meissner E, Richter G (2005) The challenge to the automotive battery industry: the battery has to become an increasingly integrated component within the vehicle electric power system. *J Power Sources* 144(2):438–460
- Milo A, Gaztanaga H, Etxeberria-Otadui I, Bilbao E, Rodriguez P (2009) Optimization of an experimental hybrid microgrid operation: reliability and economic issues. *IEEE Bucharest Power Tech Conference*, Bucharest, Romania, 28 June–2 July 2009, pp 1–6
- Noruzi A et al (2015) A new method for probabilistic assessments in power systems, combining monte carlo and stochastic-algebraic methods. *Complexity* 21(2):100–110

- Tsekouras GJ, Hatziargyriou ND, Dialynas EN (2006) An optimized adaptive neural network for annual midterm energy forecasting. *IEEE Trans Power Syst* 21(1):385–391
- Usman Iftikhar M, Riu D, Druart F, Rosini S, Bultel Y, Retière N (2006) Dynamic modeling of proton exchange membrane fuel cell using noninteger derivatives. *J Power Sources* 160(2):1170–1182
- Valenciaga F, Puleston PF (2005) Supervisor control for a stand-alone hybrid generation system using wind and photovoltaic energy. *IEEE Trans Energy Convers* 20(2):398–405
- Zou J, Shu J, Zhang Z, Luo W (2014) An active power allocation method for wind-solar-batteries hybrid power system. *Electric Power Components Syst* 42:1530–1540